Recent Insights into the Physics of the Sun and Heliosphere: Highlights from SOHO and Other Space Missions
IAU Symposium, Vol. 203, 2001
P. Brekke, B. Fleck, and J. B. Gurman eds.

Non-ideal MHD Properties of Photospheric Flux Tubes

J. Kleimann

Theoretische Physik IV, Ruhr-Universität, 44780 Bochum, Germany

G. Hornig

Theoretische Physik IV, Ruhr-Universität, 44780 Bochum, Germany

Abstract. Magnetic flux tubes reaching from the solar convection zone into the chromosphere have to pass through the relatively cool, and therefore highly non-ideal (i.e. resistive) photospheric plasma. It is shown that stationary MHD equilibria of magnetic flux tubes which pass through this region require an inflow of plasma into the tube and a deviation from isorotation along the tube axis. Although for characteristic parameters of thick flux tubes the effect is negligible, a scaling law indicates its importance for small-scale structures. The relevance of this inflow for the expansion of flux tubes above the photosphere is discussed.

1. Introduction

The interaction of solar flux tubes with the surrounding plasma is usually treated in the framework of *ideal magnetohydrodynamics (MHD)*, i.e. with resistivity $\eta = 0$. While this approach appears to be well suited for both the convection zone and the upper chromosphere, it becomes doubtful for the relatively cold and thus almost neutral photosphere (see Fig. 1). The purpose of this work is to compute the deviation from the behaviour known from ideal MHD in a self-consistent manner. To this end, we assume a given variation of plasma temperature with height and compute the resulting mass flows associated with an arch-shaped tube that passes this region. To see how the coupling is affected by the non-ideality, we keep the tube summit fixed and impose stationary vortexes at the footpoints. For simplicity, we restrict ourselves to *stationary* solutions for only *one* of the tube's two footpoints (thereby ignoring its loop-like global geometry) and try to infer the overall tube properties from more qualitative reasoning.

2. Equations and Coordinates Used

The ensuing calculations will use cylindrical coordinates $[r, \phi, z]$, with unit vectors $[\mathbf{e}_r, \mathbf{e}_\phi, \mathbf{e}_z]$. The $(z = 0)$–plane is given by the photosphere's lower boundary, while the z–axis coincides with the tube axis and is pointing away from the Sun's core. The problem's axial symmetry is then incorporated via $\partial_\phi = 0$. With $\partial_t = 0$, the set of MHD vector equations to be solved for the mass flow

https://doi.org/10.1017/S0074180900219888 Published online by Cambridge University Press

velocity $\mathbf{v}$ and the electromagnetic fields $\mathbf{B}$ and $\mathbf{E} =: -\nabla\Phi$ are as follows:

$$
\begin{aligned}
0 &= -\nabla P + \mathbf{j}\times\mathbf{B} + \rho\,\mathbf{g} && (1)\\
\eta\,\mathbf{j} &= -\nabla\Phi + \mathbf{v}\times\mathbf{B} && (2)\\
\mu\,\mathbf{j} &= \nabla\times\mathbf{B} && (3)\\
0 &= \nabla\cdot\mathbf{B} && (4)\\
0 &= \nabla\cdot(\rho\,\mathbf{v}) && (5)
\end{aligned}
$$

with ρ and η denoting the plasma's mass density and resistivity, respectively. The inertia term $\rho(\mathbf{v}\cdot\nabla)\mathbf{v}$ is omitted from (1) since its ratio to the induction term is of order $\mathcal{O}[(v/v_\mathrm{A})^2]$, where $v_\mathrm{A} := B/\sqrt{\mu\rho}$ is the *Alfvén* velocity. Observation indicates $(v/v_\mathrm{A})^2 \approx 0.03 \ll 1$ inside a photospheric tube.

3. Resistive Inflow towards the Tube Axis

Denoting by $\mathbf{v}_\mathrm{p}$ and $\mathbf{B}_\mathrm{p}$ the poloidal components of $\mathbf{v}$ and $\mathbf{B}$, and defining

$$\mathbf{e}_{||} := \mathbf{B}_\mathrm{p}\;/\;\|\mathbf{B}_\mathrm{p}\| \quad\text{and}\quad \mathbf{e}_\perp := \mathbf{e}_\phi\times\mathbf{e}_{||} \tag{6}$$

one can use (2) to show that the component of $\mathbf{v}$ *normal* to the tube surface is

$$\mathbf{v}_\perp := (\mathbf{v}_\mathrm{p}\cdot\mathbf{e}_\perp)\;\mathbf{e}_\perp = [\eta(\mathbf{x})/\mu]\left[\nabla(\ln\|\mathbf{B}_\mathrm{P}\|)\cdot\mathbf{e}_\perp - (\nabla\times\mathbf{e}_{||})\cdot\mathbf{e}_\phi\right]\;\mathbf{e}_\perp\,. \tag{7}$$

Since for a flux tube $\|\mathbf{B}_\mathrm{P}\|$ by definition decreases outwards, there will be an *inflow* of matter into the tube throughout the entire region where $\eta \neq 0$ in the case of a straight tube (where $\nabla\times\mathbf{e}_{||} = \mathbf{0}$), or, more general, in the generic case (where the contribution from the $(\nabla\times\mathbf{e}_{||})$ term is small). It is evident that $\mathbf{B}_\mathrm{P} \to \pm\alpha\;\mathbf{B}_\mathrm{P}$ will leave $\mathbf{v}_\perp$ unchanged for any constant α. Taking $\mathcal{R}$ as the tube's typical radius, we see that $\|\mathbf{v}_\perp\| \propto 1/\mathcal{R}$, which implies that the total mass inflow $\dot{M} = \int_{\{r=R\}}(\rho\;\mathbf{v}_\perp)\cdot\mathbf{da} \propto \int_{z_\mathrm{D}}^{z_\mathrm{D}+\Delta z}[\rho(z)\eta(z)/R]\;\,2\pi R\;dz$ occurring within the layer $z \in [z_D, z_D+\Delta z]$ is *scale-independent with respect to R,* i.e. tubes of various radii (but with the same B–profile) transport the same mass rate, regardless of their strength. (With the data of section 4., we find a total mass inflow rate of $\dot{M} \approx 2.7\cdot10^6$ kg/s.)

Since the inflowing plasma cannot leave the tube outside the non-ideal zone, we are forced to conclude that either a) a steady increase of tube diameter occurs (tube gets "inflated") or b) the tube is static, thereby enforcing downflow into the convection zone. Although the present model does not allow for a definite answer, recent observations (Watko & Klimchuk 1999) seem to favour the downflow alternative. More sophisticated explanations (involving, for instance, radial ionisation gradients) are well conceivable but clearly beyond the scope of this simple model.

4. Quantitative Evaluation of the Complete Flow

Specialising on tubes that are of cylindrical shape near the footpoints, one can use eq. (1) and (4) to show that $\partial_r P(r,z) = 0 = \partial_r\rho(r,z)$, $\mathbf{B} = \mathbf{B}(r)$ and hence

$$\mathbf{j}\times\mathbf{B} \equiv \mathbf{0} \tag{8}$$

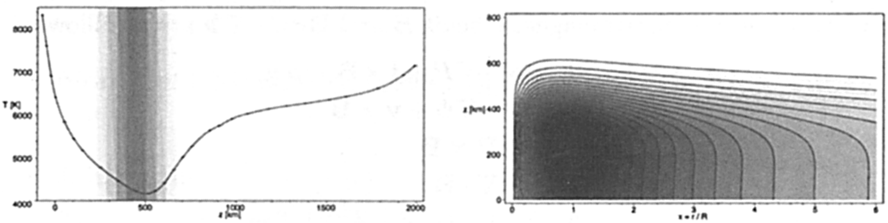

Figure 1. Left: temperature variation with z and the embedded resistive layer (shaded). Right: Contour plot of $v_\phi(x,z)$. The footpoint vortex profile is $v_\phi(x,0)/(80 \text{ m/s}) \approx (R/100 \text{ km})^{-2}\, x/(1+x^2)$.

for *arbitrary* equations of state $P = P[\rho, T]$. *A cylindrical flux tube has to be force-free if the temperature of the ambient medium is horizontally stratified.* Assuming for simplicity that we have the same vortex with the proper orientation at both footpoints implies $\mathbf{v} = \mathbf{0}$ at the summit ($z = z_{\rm sm}$). In this case we have

$$\left[\begin{array}{lcl} v_r(x,z) & = & -(R^{-1})\ \beta_1(\mathbf{B}_{\rm ff})\ \eta(z) \\ v_\phi(x,z) & = & \pm(R^{-2})\ [\beta_2(\mathbf{B}_{\rm ff}) I_2(z) + \beta_3(\mathbf{B}_{\rm ff}) I_1(z)] \\ v_z(x,z) & = & +(R^{-2})\ \beta_4(\mathbf{B}_{\rm ff})\ I_2(z) \end{array}\right] \tag{9}$$

with $x \equiv r/R$, known functions $\beta_{1\ldots4}$ and $\mathbf{B}_{\rm ff}$ satisfying (8), while the $I_{1,2}(z)$ are defined as $I_1(z) := \int_z^{z_{\rm sm}} \eta(\zeta)\, d\zeta$ and $I_2(z) := \int_z^{z_{\rm sm}} \eta(\zeta)\, [\rho(\zeta)/\rho(z)]\, d\zeta$. In the ensuing quantifications, we specialise to $\mathbf{B}_{\rm ff} = B_0[0, x/(1+x^2), 1/(1+x^2)]$ as a "flux tube prototype" and use the $\rho(z)$ and $T(z)$ data provided by the solar atmosphere model "C" of Vernazza, Avrett, & Loeser (1981) (see Fig. 1) along with Spitzer's formula and the Saha equation to derive the corresponding η–profile. A reasonable approximation is $\eta(z) = \eta_0\ \exp[-(z-z_{\rm m})^2/L^2]$ with $\eta_0 = 0.1\ \Omega$ m, $z_{\rm m}$ =440 km and $L = 140$ km. The scaling of $\mathbf{v}$ is dominated by $v_{\phi,z}$, i.e. $\|\mathbf{v}\| \propto R^{-2}$. The toroidal flow depicted in Fig. 2 shows a striking deviation from the flow expected for the case $\eta = 0$ (in which *iso-rotation* forces $\Omega(x,z) := v_\phi(x,z)/(xR)$ to be constant along field lines, i.e. $\partial_z \Omega \equiv 0$). Although for observable tube sizes ($R \gtrsim 100$ km) $\|\mathbf{v}\|$ is still too low to be distinguished from the motions of the ambient plasma, further improvement in image resolution might render observational verification feasible.

References

Watko, J., Klimchuk, J. 2000, SoPh, 193, 77

Vernazza, J., Avrett, E., & Loeser, R. 1981 ApJS, 45, 635